Conflict Analysis for Cooperative Merging Using V2X Communication

Hao M. Wang*, Tamás G. Molnár*, Sergei S. Avedisov†, Ahmed H. Sakr†, Onur Altintas†, and Gábor Orosz*,‡
*Department of Mechanical Engineering, University of Michigan, Ann Arbor, MI 48109, USA
Email: {haowangm, molnart, orosz}@umich.edu
†Toyota Motor North America R&D - InfoTech Labs, Mountain View, CA 94043, USA
Email: {sergei.avedisov, ahmed.sakr, onur.altintas}@toyota.com
‡Department of Civil and Environmental Engineering, University of Michigan, Ann Arbor, MI 48109, USA

***Abstract*— In this paper we investigate the problem of a vehicle merging to a main road while another vehicle is approaching on that road. We utilize conflict analysis to help the decision making and control for vehicles of different automation levels. We demonstrate that using vehicle-to-everything (V2X) communication, e.g., basic safety message (BSM), we are able to prevent conflict between the two vehicles. We design a longitudinal controller for the merging vehicle and show that V2X communication is also beneficial in improving the time efficiency of the merge. The results are demonstrated by performing simulations based on real highway data.**

I. Introduction

Merging remains one of many challenging traffic scenarios for both human-driven and automated vehicles [1], [2]. Vehicle-to-everything (V2X) communication technologies [3]–[5] may be used to benefit the safety and performance of such maneuvers according to multiple metrics. If all vehicles were automated one could deploy a large variety of control techniques to ensure the safety of road participants [6]–[11]. However, such assumptions will not hold on public roads for many years or decades, which demands techniques that are applicable when some of the vehicles are driven by humans. In this paper we assume that all vehicles are equipped with V2X connectivity and call them connected human-driven vehicles (CHVs) and connected automated vehicles (CAVs). We remark that the term CAV may stand for different levels of automation.

We define conflict between two vehicles as an event when they appear at the same location at the same time. Since vehicles have finite dimensions we define a conflict zone of finite size. In case of a merge maneuver this zone can be fixed to the ground around the location where the merging vehicle moves to the lane of the main road; see Fig. 1(a)-(c). Thus, to prevent conflict we must avoid the two vehicles to be present in the conflict zone at the same time. We remark that preventing conflicts shall improve the safety of vehicles though ensuring safety under all circumstances may require additional considerations.

In this paper, we look at conflict prevention from the perspective of the merging vehicle since, according to the traffic rules, this vehicle must yield to those approaching on the main road. We assume that the merging vehicle receives basic safety message (BSM) (containing GPS position and speed) from a vehicle approaching on the main road via

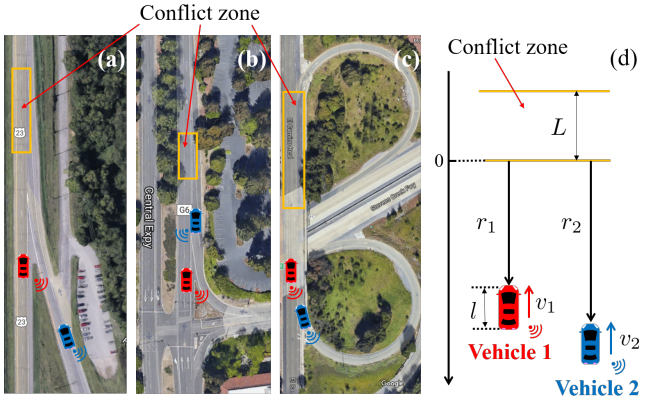

Fig. 1. Merge scenarios including (a) highway on-ramp, (b) expressway entrance, and (c) highway off-ramp; (d) the generalized model of a merge that can be used to represent scenarios (a-c).

V2X communication and utilizes this information to decide whether to merge ahead or behind the approaching vehicle. When the approaching vehicle is human-driven, one may construct probabilistic models to predict its behavior [12], [13]. In our work, rather than relying on statistical accuracy, we consider the performance limits of both vehicles and analytically calculate the so-called nonconflict, conflict and uncertain domains in the state space for both the merging ahead and merging behind cases. The corresponding conflict charts enable fast and reliable decision making for the merging vehicle.

Based on the conflict analysis we derive the minimal V2X communication range which can guarantee a conflict-free merge independent of the vehicles' initial states. Furthermore, assuming that the merging vehicle is a CAV, we design a longitudinal controller that guarantees that no conflict happens. We also demonstrate that even a single BSM packet may prevent conflict and the time efficiency can be improved by incorporating more information. The performance of the proposed controller is demonstrated by using traffic data taken from a highway in south-east Michigan.

II. Modeling Merge Dynamics

Consider the scenarios shown in Fig. 1(a)-(c) where vehicle 2 (blue) is joining the main road while vehicle 1 (red) is approaching along the main road. The conflict zones

TABLE I

PARAMETERS VALUES USED IN THE PAPER.

L	20 [m]	$v_{\min,1}$	20 [m/s]
l	5 [m]	$v_{\min,2}$	0 [m/s]
$a_{\min,1}$, $a_{\min,2}$	8 [m/s^2]	$v_{\max}$	35 [m/s]
$a_{\max,1}$, $a_{\max,2}$	4 [m/s^2]		

are located towards the end of the ramps as indicated by the yellow rectangles. The length of the conflict zone is a parameter representing a safe distance between the vehicles which may vary according to the road configuration. To simplify the matter, we ignore the lateral dynamics of both vehicles and consider the model shown in Fig. 1(d). The distances of the vehicles from the conflict zone are denoted by r_1 and r_2 while their longitudinal velocities are v_1 and v_2, respectively. The length of the conflict zone is denoted by L, the length of both vehicles is l, and we define $s := L + l$.

By neglecting the air resistance and the rolling resistance, the longitudinal dynamics of the vehicles can be given by

$$\begin{aligned} \dot{r}_1 &= -v_1, \\ \dot{v}_1 &= \mathrm{sat}(u_1), \\ \dot{r}_2 &= -v_2, \\ \dot{v}_2 &= \mathrm{sat}(u_2), \end{aligned} \tag{1}$$

where the dot represents the derivative with respect to time t. Notice that the negative signs appear since both vehicles are traveling towards the negative direction. Moreover, u_1 and u_2 represent the control inputs and the saturation function is included to model the acceleration limits of the vehicles. Assuming that the velocity is between the assigned limits $v \in (v_{\min}, v_{\max})$ we have

$$\mathrm{sat}(u) = \begin{cases} -a_{\min} & \text{if } u \in (-\infty, -a_{\min}], \\ u & \text{if } u \in (-a_{\min}, a_{\max}), \\ a_{\max} & \text{if } u \in [a_{\max}, \infty). \end{cases} \tag{2}$$

For $v = v_{\min}$, we substitute $-a_{\min}$ with 0, since the vehicle is not allowed to decelerate. Similarly, when $v = v_{\max}$, we substitute $a_{\max}$ with 0, since the vehicle is not allowed to accelerate. We remark that the acceleration limits $a_{\min,1}, a_{\min,2}, a_{\max,1}, a_{\max,2}$ and the speed limits $v_{\min,1}, v_{\min,2}, v_{\max,1}, v_{\max,2}$ may be different for different vehicles. However, for simplicity, we consider a uniform speed limit $v_{\max}$; see Table I where all parameter values are listed. Also notice that $v_{\min,2}$ is set to zero, that is, the merging vehicle is allowed to stop along the ramp.

Now we define the state as

$$x := \begin{bmatrix} r_1 & v_1 & r_2 & v_2 \end{bmatrix}^\top \in \Omega, \tag{3}$$

where $\Omega := [-s, \infty) \times [v_{\min,1}, v_{\max}] \times [-s, \infty) \times [0, v_{\max}]$. These states can be made available for both vehicles via V2X connectivity. However, when designing the decision making and control algorithms for the merging vehicle one can only prescribe the input u_2 but does not have knowledge about u_1 (except for its saturation limits $a_{\min,1}, a_{\max,1}$). These assumptions render system (1) uncontrollable, and our goal is to ensure via u_2 that the vehicles do not appear in the conflict zone at the same time.

III. CONFLICT ANALYSIS

In this section, we provide a rigorous definition of conflict using mathematical logic and the model constructed above. Then, we calculate the domains of different qualitative behavior in the state space and represent them as conflict charts. Finally, we determine communication range requirements for conflict prevention.

As mentioned above, a conflict occurs if both vehicles appear in the conflict zone at the same time. This can be formalized as the proposition

$$C := \{\exists t, r_1(t) \in (-s, 0) \wedge r_2(t) \in (-s, 0)\}, \tag{4}$$

and a nonconflicting highway merge is given by

$$\neg C = \{\forall t, r_1(t) \notin (-s, 0) \vee r_2(t) \notin (-s, 0)\}, \tag{5}$$

where we use the symbols $\wedge$ (and), $\vee$ (or), and $\neg$ (negation). This definition can be generalized for more than two vehicles and for different traffic scenarios.

We can decouple $\neg C$ into two cases where vehicle 2 on the ramp merges ahead of and behind of vehicle 1 on the main road:

$$\begin{aligned} P &:= \{\forall t, r_1(t) = 0 \implies r_2(t) \leq -s\}, \\ Q &:= \{\forall t, r_1(t) = -s \implies r_2(t) \geq 0\}. \end{aligned} \tag{6}$$

Proposition P describes that by the time vehicle 1 enters the conflict zone, vehicle 2 has already passed it, while proposition Q states that by the time vehicle 1 passes the conflict zone, vehicle 2 has not yet entered it. Furthermore, one can show that the relationship $P \vee Q \iff \neg C$ holds, leading to the definition of nonconflicting merge.

Definition 1: Given the dynamics (1), a merge is nonconflicting if proposition P or proposition Q is true. ■

Again, this definition may be extended to more than two vehicles by defining pairwise conflicts and can be generalized to a large variety of traffic scenarios.

Proposition P can be decomposed into three cases:

(1) Nonconflict case with respect to P: vehicle 2 is able to merge ahead without conflict independent of the motion of vehicle 1.
(2) Uncertain case with respect to P: vehicle 2 may be able to merge ahead without conflict depending on the motion of vehicle 1.
(3) Conflict case with respect to P: vehicle 2 is not able to merge ahead without conflict independent of the motion of vehicle 1.

Mathematically these can be formulated as disjoint sets in the state space:

$$\mathcal{A}_P := \{x(0) \in \Omega | \forall u_1(t), \exists u_2(t), P \text{ for } t > 0\}, \tag{7}$$

$$\begin{aligned} \mathcal{B}_P := \{x(0) \in \Omega | (\exists u_1(t), \forall u_2(t), \neg P \text{ for } t > 0) \wedge \\ (\exists u_1(t), \exists u_2(t), P \text{ for } t > 0)\}, \end{aligned} \tag{8}$$

$$\mathcal{C}_P := \{x(0) \in \Omega | \forall u_1(t), \forall u_2(t), \neg P \text{ for } t > 0\}. \tag{9}$$

Similarly, Proposition Q can be decomposed into nonconflict, uncertain and conflict cases, considering merge behind

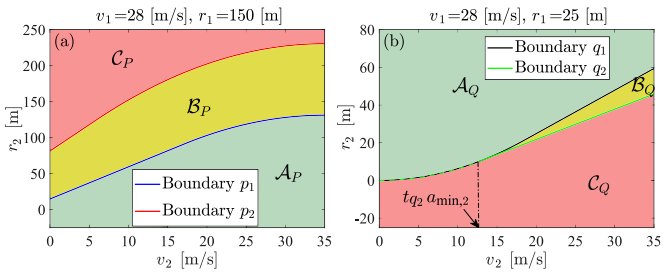

Fig. 2. Boundaries in the (v_2, r_2) plane for given v_1, r_1 values as indicated. (a) Boundaries p_1 and p_2 separating sets $\mathcal{A}_P$, $\mathcal{B}_P$, and $\mathcal{C}_P$. (b) Boundaries q_1 and q_2 separating sets $\mathcal{A}_Q$, $\mathcal{B}_Q$, and $\mathcal{C}_Q$.

instead of merge ahead, that is,

$$\mathcal{A}_Q := \{x(0) \in \Omega | \forall u_1(t), \exists u_2(t), Q \text{ for } t > 0\}, \tag{10}$$

$$\mathcal{B}_Q := \{x(0) \in \Omega | (\exists u_1(t), \forall u_2(t), \neg Q \text{ for } t > 0) \wedge (\exists u_1(t), \exists u_2(t), Q \text{ for } t > 0)\}, \tag{11}$$

$$\mathcal{C}_Q := \{x(0) \in \Omega | \forall u_1(t), \forall u_2(t), \neg Q \text{ for } t > 0\}. \tag{12}$$

Note that the first and second predicates in (8) are the negation of the predicates in (7) and (9), that is,

$$\begin{aligned} (\exists u_1, \forall u_2, \neg P) &\iff \neg(\forall u_1, \exists u_2, P), \\ (\exists u_1, \exists u_2, P) &\iff \neg(\forall u_1, \forall u_2, \neg P), \end{aligned} \tag{13}$$

implying that $\mathcal{A}_P$, $\mathcal{B}_P$, and $\mathcal{C}_P$ are pairwise disjoint and giving $\mathcal{A}_P \cup \mathcal{B}_P \cup \mathcal{C}_P = \Omega$. Similar relationships also exist in (10)–(12).

A. Conflict Charts

Using the model (1,2), one can calculate analytically the boundaries between the domains $\mathcal{A}_P$, $\mathcal{B}_P$, and $\mathcal{C}_P$ in state space, and the same holds for $\mathcal{A}_Q$, $\mathcal{B}_Q$, and $\mathcal{C}_Q$. By superimposing these boundaries we can create conflict charts that separate the state space into nonconflict, uncertain, and conflict domains.

Let us first focus on the sets $\mathcal{A}_P$, $\mathcal{B}_P$, and $\mathcal{C}_P$. If $r_1(0) \in [-s, 0]$, vehicle 1 starts in the conflict zone and vehicle 2 has no chance to merge ahead without conflict. When $r_1(0) \in (0, \infty)$, we can describe two boundaries, $r_2 = p_1(r_1, v_1, v_2)$ and $r_2 = p_2(r_1, v_1, v_2)$, which are visualized in the (v_2, r_2) plane in Fig. 2(a). These boundaries are derived by considering that by the time vehicle 1 enters the conflict zone vehicle 2 just exits assuming $[u_1(t)\ u_2(t)]^\top \equiv [a_{\max,1}\ a_{\max,2}]^\top$ and $[u_1(t)\ u_2(t)]^\top \equiv [-a_{\min,1}\ a_{\max,2}]^\top$; see Appendix I.

It can be proven that $p_2(r_1, v_1, v_2) > p_1(r_1, v_1, v_2)$, $\forall r_1 \in (0, \infty), v_1 \in [v_{\min,1}, v_{\max}], v_2 \in [0, v_{\max}]$. Thus, the regions $\mathcal{A}_P$, $\mathcal{B}_P$, and $\mathcal{C}_P$ are given by

$$\mathcal{A}_P = \{x \in \Omega | r_2 \leq p_1(r_1, v_1, v_2)\}, \tag{14}$$

$$\mathcal{B}_P = \{x \in \Omega | p_1(r_1, v_1, v_2) < r_2 \leq p_2(r_1, v_1, v_2)\}, \tag{15}$$

$$\mathcal{C}_P = \Omega \setminus (\mathcal{A}_P \cup \mathcal{B}_P). \tag{16}$$

These regions are highlighted in Fig. 2(a) with green, yellow, and red shading.

Likewise, we consider the sets $\mathcal{A}_Q$, $\mathcal{B}_Q$, and $\mathcal{C}_Q$. There are two boundaries related to proposition Q:

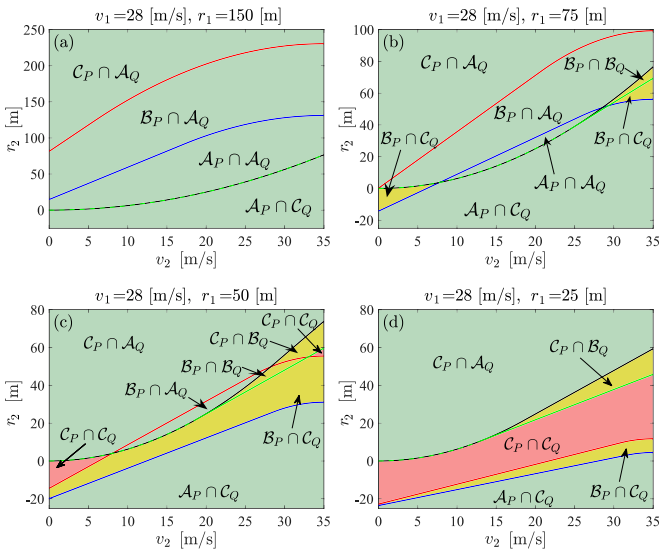

Fig. 3. Conflict charts for given v_1, r_1 values, where each region is an intersection of sets $\mathcal{A}_P$, $\mathcal{B}_P$, and $\mathcal{C}_P$ and sets $\mathcal{A}_Q$, $\mathcal{B}_Q$, and $\mathcal{C}_Q$.

$r_2 = q_1(r_1, v_1, v_2)$ and $r_2 = q_2(r_1, v_1, v_2)$; see Fig. 2(b). These are calculated by considering that by the time vehicle 1 exits the conflict zone vehicle 2 just enters it assuming $[u_1(t)\ u_2(t)]^\top \equiv [-a_{\min,1}\ -a_{\min,2}]^\top$ and $[u_1(t)\ u_2(t)]^\top \equiv [a_{\max,1}\ -a_{\min,2}]^\top$. Note that boundaries q_1 and q_2 overlap for $v_2 \in [0, t_{q2} a_{\min,2}]$, where t_{q2} represents the time needed for vehicle 1 to exit the conflict zone, with $u_1(t) \equiv a_{\max,1}$; see (35) in Appendix I. One can then prove that, $q_1(r_1, v_1, v_2) > q_2(r_1, v_1, v_2)$, $\forall r_1 \in [-s, \infty)$, $v_1 \in [v_{\min,1}, v_{\max}]$, $v_2 \in (t_{q2} a_{\min,2}, \infty)$. Thus, the regions $\mathcal{A}_Q$, $\mathcal{B}_Q$, and $\mathcal{C}_Q$ are

$$\mathcal{A}_Q = \{x \in \Omega | r_2 \geq q_1(r_1, v_1, v_2)\} \tag{17}$$

$$\mathcal{B}_Q = \{x \in \Omega | q_2(r_1, v_1, v_2) \leq r_2 < q_1(r_1, v_1, v_2)\}, \tag{18}$$

$$\mathcal{C}_Q = \Omega \setminus (\mathcal{A}_Q \cup \mathcal{B}_Q). \tag{19}$$

These regions are shaded as green, yellow, and red in Fig. 2(b).

Having introduced the boundaries and regions related to P and Q separately, let us now combine them together. In Fig. 3(a)-(d), we plot the boundaries for $v_1 = 28$[m/s] and different r_1 values as indicated. Each region in these graphs is given by the intersection of a set related to P and a set related to Q. We color the regions as follows: combining a green region with any other region gives green; combining a yellow region with a yellow or red region gives yellow; combining two red regions gives red. Note that the sequence of these charts illustrates the evolution of the boundaries while vehicle 1 approaches the conflict zone with constant speed. We refer to these as conflict charts.

B. Communication Range

For initial conditions $x(0) \in \mathcal{A}_P \cup \mathcal{A}_Q$ in the green region, there exists a controller $u_2(t)$ such that conflict can be prevented for $t > 0$, that is, $x(t) \in \mathcal{A}_P \cup \mathcal{A}_Q$. The following theorem relates this to a communication range requirement.

Theorem 1: The statement $x(0) \in \mathcal{A}_P \cup \mathcal{A}_Q$ holds if $r_1(0) \geq r_1^*$ where

$$r_1^* = \max\{\underline{r}_1, \overline{r}_1\}, \tag{20}$$

and

$$\underline{r}_1 = \begin{cases} \sqrt{\frac{2s}{a_{\max,2}}}v_{\max}, & \text{if} \quad s\,a_{\max,2} \leq \frac{1}{2}v_{\max}^2, \\ s + \frac{v_{\max}^2}{2a_{\max,2}}, & \text{otherwise}, \end{cases} \tag{21}$$

$$\overline{r}_1 = s + \frac{v_{\max}^2}{2a_{\min,2}}. \tag{22}$$

Proof: See Appendix II. ∎

This implies that if vehicle 2 receives a single V2X packet from vehicle 1 when vehicle 1 is at least r_1^* distance away from the conflict zone, then independent of the initial state $x(0)$ and $u_1(t)$, $t \geq 0$, there exists a controller $u_2(t)$, $t \geq 0$ such that it prevents conflict for $t > 0$. For the parameters given in Table I, we have $r_1^* = 124$ [m] which is easy to satisfy with current V2X technologies.

IV. Controller Design

Based on the conflict analysis above here we design a controller for the merging vehicle which can guarantee that no conflict occurs. While the analysis above holds for vehicles of different levels of automation, here we assume the merging vehicle 2 to be automated (i.e., a CAV) which is necessary to implement the controller. On the other hand, no automation is needed for vehicle 1 approaching on the main road so we consider it to be human-driven (i.e., a CHV). Finally, we assume that the communication range requirement given in Theorem 1 holds, i.e., the CAV receives at least one packet of motion information from the CHV before the CHV reaches the distance r_1^* from the conflict zone.

To ensure a nonconflicting highway merge independent of the CHV's control action $u_1(t)$, we propose the controller

$$u_2(t) = \begin{cases} u_2^{\mathcal{A}_P}, & \text{if } x(0) \in \mathcal{A}_P, \\ u_2^{\mathcal{A}_Q}, & \text{otherwise}, \end{cases} \tag{23}$$

for $t \geq 0$, where $t = 0$ is set when the CAV receives the first packet from the CHV. Here, $u_2^{\mathcal{A}_P}$ ensures that the CAV merges ahead of the CHV without conflict, and $u_2^{\mathcal{A}_Q}$ ensures that the CAV merges behind the CHV without conflict. Note that (23) implies that for $x(0) \in \mathcal{A}_P \cap \mathcal{A}_Q$, we still use $u_2^{\mathcal{A}_P}$ because merging ahead means higher time-efficiency for the CAV. A block diagram summarizing the decision making and control logic for the CAV is shown in Fig. 4, where the design of $u_2^{\mathcal{A}_Q}$ is divided into several cases as discussed below.

When merging ahead of the CHV the constant control input

$$u_2^{\mathcal{A}_P} = a_{\max,2}, \tag{24}$$

is chosen since it makes the CAV's merge the most time-efficient while it also ensures that no conflict occurs. Note that according to the saturation function (2) in (1), the CAV's acceleration becomes zero once its velocity reaches $v_{\max}$.

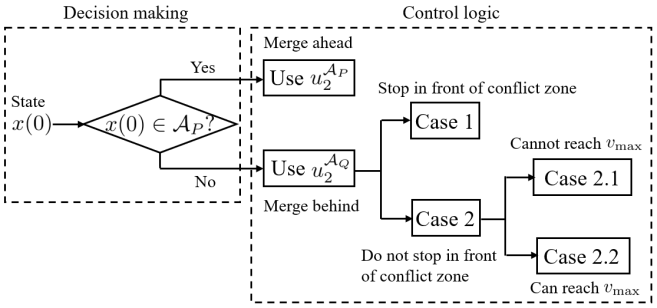

Fig. 4. Block diagram of the decision making and control logic of the CAV under the communication requirement in Theorem 1.

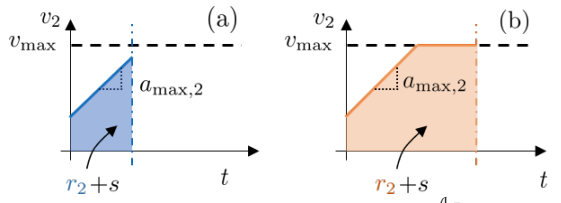

Fig. 5. Velocity profiles when applying controller $u_2^{\mathcal{A}_P}$. (a) speed limit $v_{\max}$ is not reached; (b) speed limit $v_{\max}$ is reached.

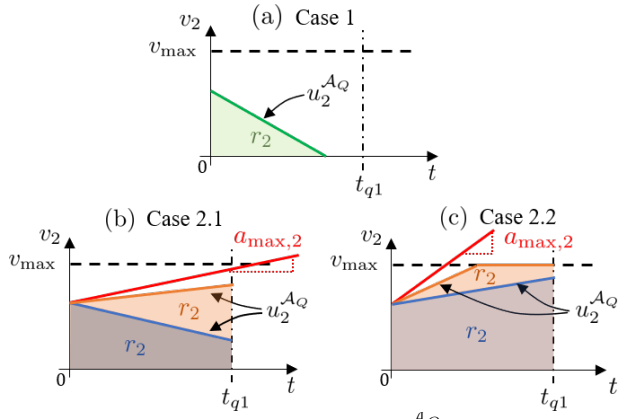

Fig. 6. Velocity profiles for the controller $u_2^{\mathcal{A}_Q}$. The different panels correspond to the cases in Fig. 4.

Figure 5 shows two different velocity profiles when $u_2^{\mathcal{A}_P}$ is applied to pass the conflict zone. Panels (a) and (b) correspond to cases where $v_{\max}$ is not reached and where it is reached, respectively, before the CAV clears the conflict zone.

When merging behind the CHV, the constant control input $u_2^{\mathcal{A}_Q}$ is proposed for the CAV to ensure that no conflict occurs regardless of $u_1(t)$. Thus, we assume the worst case scenario that the CHV applies $u_1(t) = -a_{\min,1}$ and it clears the conflict zone by time t_{q1}; see Appendix I. For $t < t_{\mathrm{q1}}$ the CAV shall stay outside of the conflict zone. To maximize the CAV's time efficiency we choose $u_2^{\mathcal{A}_Q}$ such that the CAV arrives at the front edge of conflict zone at time t_{q1}.

For simplicity we drop the (0) when referring to the initial values of the state x. That is, we use r_1, v_1, r_2, v_2 instead of $r_1(0), v_1(0), r_2(0), v_2(0)$. We distinguish the following two cases.

Case 1: $r_2 \leq \frac{1}{2}t_{\mathrm{q1}}v_2 \implies$ the CAV must stop at the

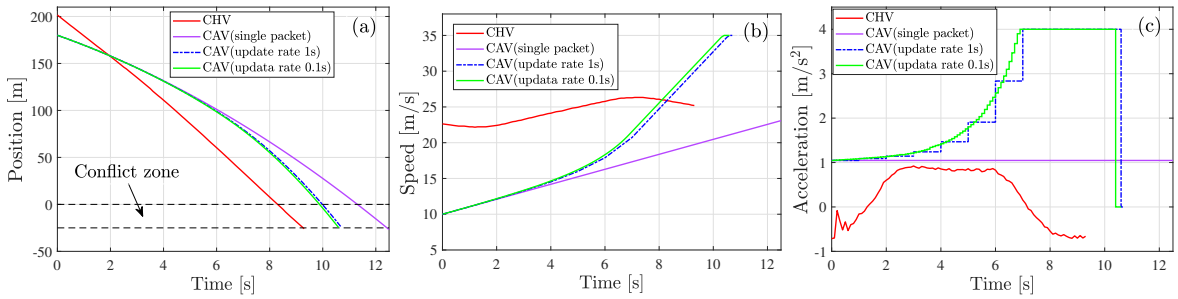

Fig. 7. Simulation results using real traffic data for the CHV (red) when applying (25), (26), and (27) to control the CAV with different packet update rates (purple, blue, green). The initial state of the CAV is given by $r_2(0) = 180[\text{m}]$, $v_2(0) = 10[\text{m/s}]$.

front edge of the conflict zone;

Case 2. $r_2 > \frac{1}{2}t_{\text{q1}}v_2 \implies$ the CAV does not need to stop at the front edge of conflict zone, cf. Fig. 4.

For Case 1, the control input is given by

$$u_2^{\mathcal{A}_Q} = -\frac{v_2^2}{2r_2}, \tag{25}$$

which allows the CAV to stop right in front of the conflict zone before time t_{q1}; see Fig. 6(a) where the area below the curve is the distance r_2. For Case 2 there are two subcases.

Case 2.1: $a_{\max,2} < (v_{\max} - v_2)/t_{\text{q1}} \implies$ the CAV's speed cannot reach $v_{\max}$ by time t_{q1}. In this case we use

$$u_2^{\mathcal{A}_Q} = \begin{cases} \frac{2(r_2 - v_2 t_{\text{q1}})}{t_{\text{q1}}^2}, & \text{if } r_2 \in (\frac{1}{2}t_{\text{q1}}v_2, \frac{1}{2}t_{\text{q1}}^2 a_{\max,2} + v_2 t_{\text{q1}}], \\ a_{\max,2}, & \text{otherwise.} \end{cases} \tag{26}$$

Case 2.2: $a_{\max,2} \geq (v_{\max} - v_2)/t_{\text{q1}} \implies$ the CAV's speed can reach $v_{\max}$ by time t_{q1}. In this case we use

$$u_2^{\mathcal{A}_Q} = \begin{cases} \frac{2(r_2 - v_2 t_{\text{q1}})}{t_{\text{q1}}^2}, & \text{if } r_2 \in (\frac{1}{2}t_{\text{q1}}v_2, \frac{1}{2}t_{\text{q1}}(v_2 + v_{\max})], \\ \frac{(v_{\max} - v_2)^2}{2(t_{\text{q1}}v_{\max} - r_2)}, & \text{if } r_2 \in (\frac{1}{2}t_{\text{q1}}(v_2 + v_{\max}), \\ & \quad - \frac{(v_{\max} - v_2)^2}{2a_{\max,2}} + t_{\text{q1}}v_{\max}], \\ a_{\max,2}, & \text{otherwise.} \end{cases} \tag{27}$$

Note that in Case 2.2 the control input $u_2^{\mathcal{A}_Q}$ saturates once the CAV's speed reaches $v_{\max}$.

Cases 2.1 and 2.2 are explained by the velocity profiles in Fig. 6(b) and (c), respectively. Panel (b) shows Case 2.1 where the CAV cannot reach the velocity $v_{\max}$ by time t_{q1}, not even by applying the maximum acceleration $a_{\max,2}$ (red line). The CAV uses the acceleration needed to cover the distance r_2 by t_{q1} or the maximum acceleration $a_{\max,2}$ if the distance is larger than what it can cover. Panel (c) demonstrates Case 2.2 where a large enough acceleration allows the CAV to reach $v_{\max}$.

The proposed controller design guarantees that region $\mathcal{A}_P$ is invariant under $u_2^{\mathcal{A}_P}$, and $\mathcal{A}_Q$ is invariant under $u_2^{\mathcal{A}_Q}$. That is $\mathcal{A}_P \cup \mathcal{A}_Q$ is invariant under (23). Recall that $u_2^{\mathcal{A}_Q}$ is derived by using a single packet of information received from the CHV at $t = 0$ and it is assumed that the CHV is applying $u_1(t) \equiv -a_{\min,1}$ along $t > 0$. However, if the CAV receives more packets later, it may update its controller by re-calculating (25), (26), and (27) with the most recent information. It can be proven that utilizing more packets from the CHV results in a larger $u_2^{\mathcal{A}_Q}$, which means better time-efficiency for the CAV.

TABLE II

TIME NEEDED FOR THE CAV TO MERGE WITHOUT CONFLICT.

	Single packet	Update rate 1 s	Update rate 0.1 s
Time needed	12.42 [s]	10.68 [s]	10.57 [s]

We demonstrate the performance of the controller in Fig. 7 by utilizing the GPS data of a human-driven vehicle approaching an on-ramp on Highway 23 in Michigan; see Fig. 1(a). The CHV's position, velocity and acceleration are shown in red. We consider that a CAV on the ramp intends to merge and applies controller (23). At the initial time we have $x(0) \in \mathcal{B}_P \cap \mathcal{A}_Q$, so the decision to merge behind the CHV is made and the controller $u_2^{\mathcal{A}_Q}$ is used. The performance of the CAV is compared for different packet update rates as indicated by color. Indeed, time-efficiency is significantly improved when more packets are received: the CAV merges onto the highway within shorter time and with higher speed; see Table II.

V. CONCLUSION

In this paper we illustrated conflict analysis by considering a scenario where a vehicle merging onto a main road seeks to avoid conflict with a vehicle approaching on the main road. By constructing conflict charts we demonstrated that if the vehicle on the main road relays its position and speed to the merging vehicle through V2X communication before a critical distance, the merging vehicle is able to avoid conflict. Furthermore, if the merging vehicle is automated, we can use the conflict charts to design a controller that uses the BSM packet to guarantee a conflict-free merge. Lastly, we showed that if the merging vehicle receives multiple BSM packets from the main road vehicle, the time efficiency of the conflict-free merge increases with the V2X communication rate. Our future work includes the experimental validation of the proposed controller and scaling up conflict analysis for a larger numbers of vehicles.

APPENDIX I
CONFLICT CHART BOUNDARIES

Boundaries p_1 and p_2 in (14), (15), and (16) are given by

$$r_2 = p_1(r_1, v_1, v_2) = p(t_{\mathrm{p1}}, v_2), \tag{28}$$

$$r_2 = p_2(r_1, v_1, v_2) = p(t_{\mathrm{p2}}, v_2), \tag{29}$$

where

$$p(t_{\mathrm{p1}}, v_2) = \tag{30}$$
$$\begin{cases} t_{\mathrm{p1}} v_2 + \frac{1}{2} t_{\mathrm{p1}}^2 a_{\max,2} - s & \text{if } v_2 \le v_{\max} - t_{\mathrm{p1}} a_{\max,2}, \\ -\frac{(v_{\max}-v_2)^2}{2a_{\max,2}} + t_{\mathrm{p1}} v_{\max} - s & \text{if } v_2 > v_{\max} - t_{\mathrm{p1}} a_{\max,2}, \end{cases}$$

and

$$t_{\mathrm{p1}} = \begin{cases} \frac{\sqrt{v_1^2 + 2a_{\max,1} r_1} - v_1}{a_{\max,1}} & \text{if } r_1 \le \frac{v_{\max}^2 - v_1^2}{2a_{\max,1}}, \\ \frac{v_{\max}-v_1}{a_{\max,1}} + \frac{r_1 - \frac{v_{\max}^2 - v_1^2}{2a_{\max,1}}}{v_{\max}} & \text{if } r_1 > \frac{v_{\max}^2 - v_1^2}{2a_{\max,1}}, \end{cases}$$

$$t_{\mathrm{p2}} = \begin{cases} \frac{v_1 - \sqrt{v_1^2 - 2a_{\min,1} r_1}}{a_{\min,1}} & \text{if } r_1 \le \frac{v_1^2 - v_{\min,1}^2}{2a_{\min,1}}, \\ \frac{v_1 - v_{\min,1}}{a_{\min,1}} + \frac{r_1 - \frac{v_1^2 - v_{\min,1}^2}{2a_{\min,1}}}{v_{\min,1}} & \text{if } r_1 > \frac{v_1^2 - v_{\min,1}^2}{2a_{\min,1}}. \end{cases} \tag{31}$$

Note that t_{p1} and t_{p2} are the time needed for the CHV to reach the conflict zone with $u_1(t) \equiv a_{\max,1}$ and $u_1(t) \equiv -a_{\min,1}$, respectively. Thus, the relation $t_{\mathrm{p2}} > t_{\mathrm{p1}}$ always holds, and therefore, we have $p_2 > p_1$.

Boundaries q_1 and q_2 in (17), (18), and (19) are given by

$$r_2 = q_1(r_1, v_1, v_2) = q(t_{\mathrm{q1}}, v_2), \tag{32}$$

$$r_2 = q_2(r_1, v_1, v_2) = q(t_{\mathrm{q2}}, v_2), \tag{33}$$

where

$$q(t_{\mathrm{q1}}, v_2) = \begin{cases} t_{\mathrm{q1}} v_2 - \frac{1}{2} t_{\mathrm{q1}}^2 a_{\min,2} & \text{if } v_2 \ge t_{\mathrm{q1}} a_{\min,2}, \\ \frac{v_2^2}{2a_{\min,2}} & \text{if } v_2 < t_{\mathrm{q1}} a_{\min,2}, \end{cases} \tag{34}$$

and

$$t_{\mathrm{q1}} = \begin{cases} \frac{v_1 - \sqrt{v_1^2 - 2a_{\min,1}(r_1+s)}}{a_{\min,1}} & \text{if } r_1 \le \frac{v_1^2 - v_{\min,1}^2}{2a_{\min,1}} - s, \\ \frac{v_1 - v_{\min,1}}{a_{\min,1}} + \frac{r_1 + s - \frac{v_1^2 - v_{\min,1}^2}{2a_{\min,1}}}{v_{\min,1}} & \text{if } r_1 > \frac{v_1^2 - v_{\min,1}^2}{2a_{\min,1}} - s, \end{cases}$$

$$t_{\mathrm{q2}} = \begin{cases} \frac{\sqrt{v_1^2 + 2a_{\max,1}(r_1+s)} - v_1}{a_{\max,1}} & \text{if } r_1 \le \frac{v_{\max}^2 - v_1^2}{2a_{\max,1}} - s, \\ \frac{v_{\max}-v_1}{a_{\max,1}} + \frac{r_1 + s - \frac{v_{\max}^2 - v_1^2}{2a_{\max,1}}}{v_{\max}} & \text{if } r_1 > \frac{v_{\max}^2 - v_1^2}{2a_{\max,1}} - s. \end{cases} \tag{35}$$

APPENDIX II
PROOF OF THEOREM 1

Notice that boundary q_1 is upper bounded by $r_2 = f(v_2) = v_2^2/(2a_{\min,2})$. Thus, to prove that $x(0) \in \mathcal{A}_P \cup \mathcal{A}_Q$ holds for $r_1 \ge r_1^*$, it is sufficient to show that $r_1 \ge r_1^* \Rightarrow p_1(r_1, v_1, v_2) \ge f(v_2)$, $\forall v_1 \in [v_{\min,1}, v_{\max}], \forall v_2 \in [0, v_{\max}]$.

Let us define

$$\delta(r_1, v_1, v_2) := p_1(r_1, v_1, v_2) - f(v_2). \tag{36}$$

By calculating $\frac{\partial \delta}{\partial v_2}(r_1, v_1, v_2)$, one may show that δ first increases and then decreases with respect to v_2 on $[0, v_{\max}]$. That is, δ takes minimum value at $v_2 = 0$ or $v_{\max}$.

Now consider the inequalities

$$\delta(r_1, v_1, 0) \ge 0 \iff r_1 \ge g_1(v_1), \tag{37}$$

$$\delta(r_1, v_1, v_{\max}) \ge 0 \iff r_1 \ge g_2(v_1), \tag{38}$$

where g_1 and g_2 are functions of v_1. One can confirm that the $\underline{r}_1$ and $\overline{r}_1$ given in (21) and (22) correspond to the maximum values of g_1 and g_2 on $v_1 \in [v_{\min,1}, v_{\max}]$. Thus if $r_1 \ge r_1^* = \max\{\underline{r}_1, \overline{r}_1\}$, then both (37) and (38) hold independent of v_1. This yields that $\delta(r_1, v_1, v_2) \ge 0$, i.e., $p_1(r_1, v_1, v_2) \ge f(v_2)$, $\forall v_1 \in [v_{\min,1}, v_{\max}]$, $\forall v_2 \in [0, v_{\max}]$.

REFERENCES

[1] A. Kondyli and L. Elefteriadou, "Modeling driver behavior at freeway–ramp merges," *Transportation Research Record*, vol. 2249, no. 1, pp. 29–37, 2011.

[2] J. Rios-Torres and A. A. Malikopoulos, "A survey on the coordination of connected and automated vehicles at intersections and merging at highway on-ramps," *IEEE Transactions on Intelligent Transportation Systems*, vol. 18, no. 5, pp. 1066–1077, 2016.

[3] K. Abboud, H. A. Omar, and W. Zhuang, "Interworking of DSRC and cellular network technologies for V2X communications: A survey," *IEEE Transactions on Vehicular Technology*, vol. 65, no. 12, pp. 9457–9470, 2016.

[4] J. I. Ge, S. S. Avedisov, C. R. He, W. B. Qin, M. Sadeghpour, and G. Orosz, "Experimental validation of connected automated vehicle design among human-driven vehicles," *Transportation Research Part C*, vol. 91, pp. 335–352, 2018.

[5] S. S. Avedisov, G. Bansal, A. K. Kiss, and G. Orosz, "Experimental verification platform for connected vehicle networks," in *21st International Conference on Intelligent Transportation Systems*, Maui, USA, 2018, pp. 818–823.

[6] A. I. M. Medina, N. Van de Wouw, and H. Nijmeijer, "Automation of a T-intersection using virtual platoons of cooperative autonomous vehicles," in *the 18th International Conference on Intelligent Transportation Systems*, Las Palmas de Gran Canaria, Spain, 2015, pp. 1696–1701.

[7] M. R. Hafner, D. Cunningham, L. Caminiti, and D. Del Vecchio, "Cooperative collision avoidance at intersections: Algorithms and experiments," *IEEE Transactions on Intelligent Transportation Systems*, vol. 14, no. 3, pp. 1162–1175, 2013.

[8] R. Kianfar, P. Falcone, and J. Fredriksson, "Safety verification of automated driving systems," *IEEE Intelligent Transportation Systems Magazine*, vol. 5, no. 4, pp. 73–86, 2013.

[9] P. Nilsson, O. Hussien, A. Balkan, Y. Chen, A. D. Ames, J. W. Grizzle, N. Ozay, H. Peng, and P. Tabuada, "Correct-by-construction adaptive cruise control: Two approaches," *IEEE Transactions on Control Systems Technology*, vol. 24, no. 4, pp. 1294–1307, 2015.

[10] S. Bansal, M. Chen, S. Herbert, and C. J. Tomlin, "Hamilton-Jacobi reachability: a brief overview and recent advances," in *the 56th IEEE Conference on Decision and Control*, Melbourne, Australia, 2017, pp. 2242–2253.

[11] M. R. Hafner and D. Del Vecchio, "Computational tools for the safety control of a class of piecewise continuous systems with imperfect information on a partial order," *SIAM Journal on Control and Optimization*, vol. 49, no. 6, pp. 2463–2493, 2011.

[12] S. Brechtel, T. Gindele, and R. Dillmann, "Probabilistic decision-making under uncertainty for autonomous driving using continuous POMDPs," in *17th International IEEE Conference on Intelligent Transportation Systemss*, Qingdao, China, 2014, pp. 392–399.

[13] C. Dong, J. M. Dolan, and B. Litkouhi, "Intention estimation for ramp merging control in autonomous driving," in *28th IEEE Intelligent Vehicles Symposium*, Redondo, USA, 2017, pp. 1584–1589.